Misfit strain, relaxation, and band-gap shift in $Ga_xIn_{1-x}P$/InP epitaxial layers

A. Bensaada, A. Chennouf, R. W. Cochrane, J. T. Graham, and R. Leonelli
Groupe de Recherche en Physique et Technologie des Couches Minces, Université de Montréal, C.P. 6128, Succ. A, Montréal, Québec H3C 3J7, Canada

R. A. Masut
Groupe de Recherche en Physique et Technologie des Couches Minces, Ecole Polytechnique, C.P. 6079, Succ. A, Montréal, Québec H3C 3A7, Canada

(Received 1 October 1993; accepted for publication 29 November 1993)

A detailed investigation of the structural and optoelectronic properties of thick GaInP epilayers on sulfur-doped InP substrates is reported. Significant variations of the optical absorption and photoluminescence transition energies from light- and heavy-hole states are observed as a function of the epilayer composition as well as of the degree of relaxation of the misfit strain. High-resolution x-ray measurements were used to determine the Ga concentrations and the strains and indicate significant anisotropic relaxation in several films. Even small relaxations result in a significant increase in the optical linewidths and a rapid drop in the transition intensities. A model with no free parameters based on the strain Hamiltonian of Pikus and Bir provides excellent agreement with the transition energies and serves to identify unambiguously the transitions observed in the optical spectra. Within this model, isotropic in-plane relaxation produces a shift of both light- and heavy-hole energies whereas anisotropic in-plane relaxation contributes only negligibly.

I. INTRODUCTION

The epitaxial growth of a III-V semiconductor with a bulk lattice parameter different from that of the substrate induces a misfit strain into the epilayer that can be elastically accommodated by a tetragonal distortion, provided the product of the lattice mismatch and the epilayer thickness is not too large. As the mismatch or epilayer thickness increases, the epilayer will relax toward its bulk structure via the generation of misfit dislocations. For the case of (001)-oriented substrates, the dislocations are directed along [110] or [1$\bar{1}$0] and a difference in the densities of dislocations in these two directions results in a further reduction of the symmetry to orthorhombic.[1]

Isotropic strain produces a shift in the energies of the conduction and valence bands; anisotropic strain lowers the crystal symmetry and hence splits the otherwise degenerate heavy-hole V_1 and light-hole V_2 valence bands at the Γ point. Several authors have reported[2–5] the effects of misfit strain on the optical properties of $Ga_xIn_{1-x}P$/GaAs epilayers which can be grown in tension ($a_{epi}<a_s$), lattice matched ($a_{epi}=a_s$), or in compression ($a_{epi}>a_s$) with an appropriate choice of the Ga concentration. In the case of tensile strain, the energy band gap is defined by the V_2-CB (conduction band) transition, and in the case of compression by the V_1-CB transition. Asai and Oe[3] reported good agreement between experimental and theoretical results for epilayers under tension; Kuo *et al.*[4] studied the band-gap shifts for the compressively strained system. In neither study was the effect of strain relaxation on the band-gap shift included.

The objective of this paper is to demonstrate the influence of strain on the optical absorption and photoluminescence (PL) spectra of $Ga_xIn_{1-x}P$ epitaxial layers grown on heavily S-doped InP substrates. We first present an x-ray analysis of the mismatch strain and relaxation of the relatively thick $Ga_xIn_{1-x}P$ epilayers and follow with the optical spectra. Transitions between the conduction band and the light- and heavy-hole valence bands are observed in absorption and in PL. We then show that the optical data for both pseudomorphic and relaxed epilayers are in excellent agreement with the theoretically predicted values. We note that such a complete understanding of the optical behavior of relatively thick epitaxial layers is an important prerequisite for understanding the optical spectra from the carriers in confined states in strained layer superlattices and multiple quantum wells.

II. EXPERIMENTAL DETAILS

Optical absorption measurements of heterostructures grown on substrates which are not transparent in the spectral region of interest are very difficult without removing the substrate.[6] However, such a procedure is destructive and can affect the integrity and the structural properties of the samples. In order to avoid such problems, GaInP/InP epilayers have been grown on heavily S-doped InP in which the S doping causes a large increase in the substrate band gap at low temperature with little change in its lattice parameter. Optical absorption measurements are thus possible in the normally opaque region above the band gap of undoped and unstrained InP.

The $Ga_xIn_{1-x}P$/InP strained heterostructures were grown in a computer-controlled cold-wall horizontal MOCVD reactor.[7] Growth was carried out at low pressure using Pd-purified hydrogen as the carrier gas and TMIn, TMGa, and PH_3 as precursors. The substrates, LEC-InP [S doped ($n\approx10^{19}$ cm^{-3}) (001) oriented] were degreased,

 0021-8979/94/75(6)/3024/6/$6.00

TABLE I. Structural parameters of the $Ga_xIn_{1-x}P$ epilayers obtained from x-ray measurements. The strains ϵ and ϵ_{xy} are defined in Eqs. (4).

Samples	InP buffer thickness (Å)	Epilayer thickness (μm)	x (%)	R_1 (%)	R_2 (%)	ϵ (10^{-3})	ϵ_{xy} (10^{-3})
CE59*S*	2000	1.77	1.6	34	18	−0.69	−0.15
CE60*S*	2000	1.20	2.6	9.6	5.3	−1.4	−0.065
CE61*S*	2000	1.27	5.7	38	14	−2.5	−0.81
CE62*S*	2000	1.27	9.0	16	53	−3.5	2.0
CE63*S*	2000	2.0	11.6	57	73	−2.5	1.1
CF86*S*	250	0.40	9.3	3.6	13	−5.1	0.52
CF88*S*	250	0.40	7.8	1.5	1.5	−4.6	0.000
CF89*S*	250	0.43	7.6	0.7	0.6	−4.5	−0.005

rinsed, etched, and preannealed for 10 min at the growth temperature under PH_3 to remove any native oxide. A thin InP buffer layer was deposited to improve the interface quality and block sulfur diffusion but was maintained thin enough to avoid problems with the absorption measurements. GaInP epilayers were then grown with thicknesses in the range from 0.4 to 2 μm as measured using scanning electron micrography (SEM). The details of the growth and characterization techniques are described in Ref. 1 and the principal structural parameters of the samples used in this study are presented in Table I.

X-ray diffraction measurements were carried out on a Philips high-resolution five-crystal diffractometer using Cu $K_{\alpha 1}$ radiation with the monochromator aligned in its Ge(220) setting and the beam width limited by a 1 mm^2 slit at the exit of the monochromator. PL was excited by the 514.5 nm line of an Ar^+ ion laser; the PL signal was dispersed by a 1-m double spectrometer and detected by a cooled GaAs photomultiplier tube using conventional photon counting techniques. Optical absorption measurements were performed using a BOMEM DA3 Fourier transform spectrometer with a quartz-halogen source, quartz beamsplitter, and Si photoconductive detector. For both the PL and absorption measurements, the samples were mounted strain-free in a helium flow cryostat and maintained at a temperature of 7 K.

III. RESULTS

A. X-ray diffraction

Symmetric (004) rocking curves give the lattice parameter ($a_\perp$) perpendicular to the (001) surface of the sample; asymmetric (115) and (1$\bar{1}$5) rocking curves provide the (110) and (1$\bar{1}$0) plane spacings ($d_{(110)}$ and $d_{(1\bar{1}0)}$). Defining a_1, a_2, and $\bar{a}$ as the equivalent in-plane tetragonal lattice parameters according to (see Fig. 1)

$$a_1=\sqrt{2}d_{(1\bar{1}0)}, \quad a_2=\sqrt{2}d_{(110)} \quad \text{and} \quad \bar{a}=(a_1+a_2)/2, \tag{1}$$

the lattice parameter of the completely relaxed epilayer of the same composition can be calculated from these data according to[1]

$$a_{\text{rel}}=a_\perp\left(\frac{1-\nu}{1+\nu}\right)+\bar{a}\left(\frac{2\nu}{1+\nu}\right), \tag{2}$$

where ν is the Poisson ratio of the film. Comparison of a_{rel} with the experimentally determined lattice parameters of bulk $Ga_xIn_{1-x}P$ alloys[8] gives the epilayer composition which is required to calculate the strains in the [001], [110], and [1$\bar{1}$0] directions.

The relaxation R is expressed as

$$R=\frac{a_\parallel-a_{\text{sub}}}{a_{\text{rel}}-a_{\text{sub}}}, \tag{3}$$

but when the relaxation exhibits an in-plane anisotropy with respect to the ⟨110⟩ directions two relaxation parameters R_1 and R_2 [with $\bar{R}=(R_1+R_2)/2$ and $\Delta R=R_1-R_2$] are defined using the a_1 and a_2 lattice parameters from Eq. (1). Relaxation values for our samples are listed in Table I.

The (004) experimental x-ray rocking curve of sample CF89*S* is shown in Fig. 2 from which we calculate $a_\perp=5.8125$ Å. The asymmetric (115) and (1$\bar{1}$5) curves give $a_1=5.8694$ Å and $a_2=5.8696$ Å so that we find $a_{\text{rel}}=5.8426$ Å. The sample is thus almost perfectly pseudomorphic ($a_1=a_2$ within experimental resolution, R is isotropic and $<1\%$) with a Ga concentration of 7.6%. The full widths at half maximum (FWHM) of the epilayer peaks of approximately 60 arcsec for this sample are further indications of its good crystalline quality. It is to be

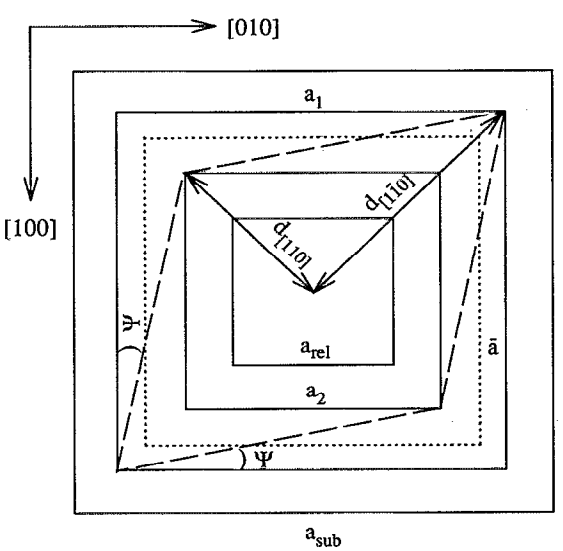

FIG. 1. Schematic of the deformation of anisotropically relaxed layers.

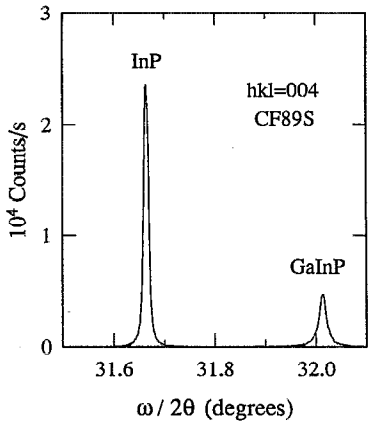

FIG. 2. X-ray diffraction curve for sample CF89*S*.

noted that other samples with anisotropic relaxations show larger x-ray peak FWHMs owing to the increasing mosaicity of the relaxed layers.[1]

B. Optical absorption and photoluminescence

The absorption edge in heavily S-doped ($\sim 10^{19}$ cm^{-3}) InP at low temperature is displaced by almost 125 meV to higher energy with respect to the undoped material; this displacement collapses to zero at room temperature. Such behavior has been previously observed in *n*-type InP samples for dopings exceeding the degenerate concentration of 10^{18} cm^{-3} and has been explained by taking into consideration the concentration-dependent effective masses, electron-electron and electron-impurity interactions.[9] However, the lattice parameter of the sulfur-doped material remains very close to that of undoped InP[10] so that subsequent InP buffer layers grow epitaxially with negligible strain.

In Fig. 3 the optical absorption spectra for all our samples are presented. These spectra are dominated by an intense peak, labeled A_2, which is followed by an absorption step. Depending on the sample, a less intense peak A_1 and absorption step or simply an absorption edge are observed at energies lower than that for A_2. The peaks A_1 and A_2 are due to the formation of excitons involving the light- or heavy-hole bands of the ternary compound. Samples grown with the 2000-Å-thick InP buffer layer have an additional absorption peak or edge at ~ 1.418 eV which is identified as arising from excitons in this buffer layer. Figure 4 shows the low-temperature PL spectra of samples CE59*S* and CF89*S*. For the first, three peaks marked P_1, P_2, and P_3 are visible: peak P_1 originates from the InP buffer layer and the two others from the GaInP epilayer. For the second, a broad and shifted (due to S diffusion[9]) InP peak P_1 and a narrow peak from the epilayer P_2 (FWHM of ~ 1 meV) are observed, as is the case for all other samples.

The effect of structural relaxation on the optical spectra can be demonstrated by combining the x-ray and optical data. The InP buffer absorption peak broadens with the relaxation and disappears completely for samples CE62*S*

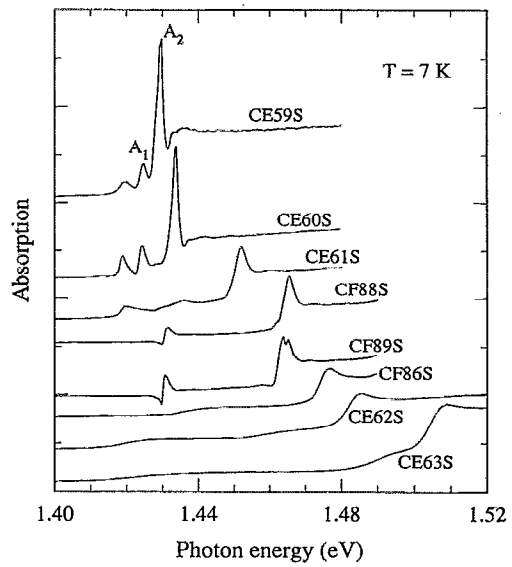

FIG. 3. Optical absorption spectra of the present samples displayed with a zero shift for clarity. Data for samples CF86*S*, CF88*S*, and CF89*S* have been multiplied by a factor of 2 for presentation purposes.

and CE63*S* where the relaxation is the largest. This behavior can be attributed to two factors. First, when the epilayer begins to relax, misfit dislocations are created at the InP/GaInP interface so that this region is certainly the most damaged. Secondly, the overall sulfur diffusion from the substrate is enhanced, probably by dislocations acting as diffusion pipes, which degrades the optical quality of the buffer layer.[11] One also notices that the intensities of the absorption peaks from the epilayers decrease with increasing layer relaxation; for large values of the relaxation, the low-energy excitonic peak disappears completely. This effect is quantified in Fig. 5 for peaks A_2 of the absorption spectra [Fig. 5(a)] and P_2 from the PL [Fig. 5(b)] where the peak linewidths are plotted as a function of the average

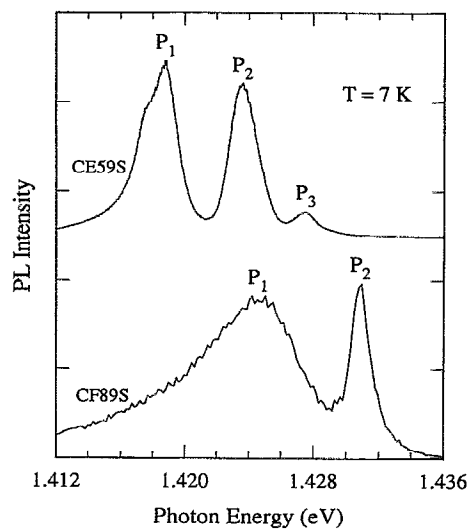

FIG. 4. Low-temperature PL of samples CE59*S* and CF89*S*.

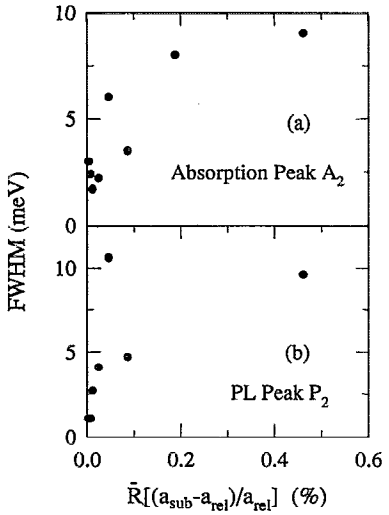

FIG. 5. Dependence of the linewidth of (a) the A_2 absorption peak and (b) the P_2 PL peak on the average strain relaxation.

in-plane deformation of the epilayer. This deformation, defined as $\bar{R}\times(a_{sub}-a_{rel})/a_{rel}$, should be proportional to the number of dislocations generated at the interface. Clearly, relaxation leads to a rapid broadening for both the optical absorption and PL peaks.

IV. ANALYSIS OF STRAIN EFFECTS ON OPTICAL PEAK ENERGIES

A. Strains in anisotropically relaxed layers

We have previously demonstrated[1] that epitaxial GaInP layers on (001) InP substrates relax by the formation of dislocations in the [110] and [1$\bar{1}$0] directions. As long as dislocations are uniformly generated in both directions the ternary layer has tetragonal symmetry; a difference in the production of dislocations in the two directions results in a lowering of the symmetry to orthorhombic. For the orthorhombic case the axes are parallel to the original [110] and [1$\bar{1}$0] directions and the original cube edges are no longer perpendicular as indicated in Fig. 1 (a similar diagram has been presented in Ref. 12). Such anisotropy in the relaxation gives rise to a shear component ϵ_{xy} of the strain. Using the a and R parameters the elements of the strain tensor are written as

$$\epsilon_{xx}=\epsilon_{yy}=-\epsilon=\frac{\bar{a}-a_{rel}}{a_{rel}}=(1-\bar{R})\,\frac{a_{sub}-a_{rel}}{a_{rel}}$$

$$=-(1-\bar{R})\epsilon^{max}, \tag{4a}$$

$$\epsilon_{zz}=2\left(\frac{c_{12}}{c_{11}}\right)\epsilon, \tag{4b}$$

$$\epsilon_{xy}=2\psi=\frac{a_1-a_2}{\bar{a}}\approx\Delta R\epsilon^{max}=\frac{\Delta R}{(1-\bar{R})}\,\epsilon, \tag{4c}$$

where ϵ^{max} is the maximum ϵ for a given Ga concentration, the c_{ij} are the elastic stiffness coefficients, and ψ is the angle of rotation of the original cube edges due to the shear strain. As defined the shear strain represents the conventional form and not the tensorial one, since the conventional form is used in the Hamiltonian cited in the next section.[13] The form for ϵ_{zz} arises from the absence of a stress component normal to the film plane. Throughout this analysis the strain components are calculated from the experimental lattice parameters and are assumed to be temperature independent since the thermal expansion coefficients of InP and $Ga_xIn_{1-x}P$ ($x<0.2$) are very close.[14]

B. Effect of strain on the optical transitions

A general approach to the analysis of the band energies involved in the optical properties of III-V semiconductors begins with the Kane Hamiltonian describing one conduction and three valence bands around the Γ point in k space. At the Γ point in a material with the zincblende structure, the valence bands including spin-orbit terms consist of a fourfold degenerate $P_{3/2}$ multiplet Γ_8 and a $P_{1/2}$ multiplet Γ_7. Within this approximation, the bands are isotropic. The application of a biaxial in-plane stress lowers the symmetry from cubic to tetragonal. As a result, all the bands are shifted in energy while the $P_{3/2}$ multiplet splits into two doublets V_1: (heavy holes, hh: $J=3/2$, $m_J=\pm 3/2$) and V_2 (light holes, lh: $J=3/2$, $m_J=\pm 1/2$) and V_2 couples with V_3 (the split-off band $P_{1/2}$).[15–17] In addition, the heavy- and light-hole bands become anisotropic with the well-known reversal of the in-plane masses of the heavy and light holes.[16] Further anisotropy and band splittings result from anisotropic in-plane stresses.[16,17]

The effect of strain on a given band at $k=0$ is derived from the orbital-strain Hamiltonian H_ϵ[13,16,17] which has the form

$$H_\epsilon=-a(\epsilon_{xx}+\epsilon_{yy}+\epsilon_{zz})-3b\left[\left(l_x^2-\frac{1}{3}l^2\right)\epsilon_{xx}+\text{c.p.}\right]$$

$$-\sqrt{3}d[(l_xl_y+l_yl_x)\epsilon_{xy}+\text{c.p.}], \tag{5}$$

where ϵ_{ij} are the components of the strain tensor, l is the angular momentum operator, and c.p. denotes cyclic permutations with respect to the indices x, y, and z. The parameter a represents the hydrostatic deformation potential; the quantities b and d are shear deformation potentials appropriate to strains of tetragonal and rhombohedral symmetries, respectively.

Combining Eqs. (4) and (5), the strain Hamiltonian H_ϵ becomes

$$H_\epsilon=\left[2a\left(\frac{c_{11}-c_{12}}{c_{11}}\right)-3b\left(\frac{c_{11}+2c_{12}}{c_{11}}\right)\left(l_z^2-\frac{1}{3}l^2\right)\right]\epsilon$$

$$+i\frac{\sqrt{3}}{2}d(l_+^2-l_-^2)\epsilon_{xy}. \tag{6}$$

$l_\pm=l_x\pm il_y$. The first two terms in Eq. (6) depend only on the average relaxation $\bar{R}$ whereas the last also involves the relaxation anisotropy ΔR. The a term produces a shift of the centers of gravity of all bands. Since only the difference between the conduction and valence band energies are measured in our experiments, only the relative hydrostatic coefficient between these bands is relevant; the a parameter

TABLE II. Parameter values at $T=0$ K for the calculation of the strain-induced energy shifts: a is the lattice parameter; c_{ij} are the elastic constants, and a, b, and d are the stress coefficients introduced in Eq. (5); Δ is the spin-orbit splitting parameter for unstrained InP.

	a (Å)	c_{11} (10^{11} dyn/cm^2)	c_{12} (10^{11} dyn/cm^2)	a (eV)	b (eV)	d (eV)	Δ (eV)
InP	5.8696	10.22[a]	5.76[a]	−7.97[a]	−1.55[a]	−4.2[c]	0.108[c]

[a]Reference 3.
[b]$a=-[(c_{11}+2c_{12})/3]\partial E_g/\partial P$, $\partial E_g/\partial P=1.1\times10^{-11}$ eV cm^2 dyn^{-1}.
[c]*Landolt–Bornstein, Numerical Data and Functional Relationships in Science and Technology* (Springer, Berlin, 1982), Group III, Vol. 17.

referred to hereafter is used in this sense. The b term is responsible for a first-order splitting of the light- and heavy-hole levels and also for a second-order coupling of the light-hole and splitting-off bands. Finally, the d term has no first-order effect at the Γ point and in second-order couples the heavy holes to both the light holes and the split-off states.

Before proceeding it is useful to examine the magnitudes of the second-order terms described above. Using the parameters in Tables I and II, we calculate that the second-order coupling between the light holes and the split-off states contributes about 6 meV to the band-gap energy for the most strained sample and will not be neglected. The leading correction arising from the coupling of the heavy holes to the light-holes via the shear term is given by

$$-\frac{d^2}{2b[(c_{11}+2c_{12})/c_{11}]}\frac{\epsilon_{xy}^2}{\epsilon}$$

and from the heavy-hole split-off coupling by

$$\frac{2d^2}{\Delta}\epsilon_{xy}^2.$$

Here Δ is the spin-orbit splitting between the split-off and light/heavy holes in the unstrained material. For sample CE62*S*, in which the shear strain is the largest, the second-order shear terms contribute less than 2 meV to the heavy-hole and light-hole band gaps; for the other samples they give less than 1 meV. Since these values are comparable to the experimental resolution of the peak positions and the energy uncertainties arising from possible errors in the estimation of the Ga concentration, we can safely neglect the effect of the shear strain for these samples. Consequently, this model predicts first- and second-order energy shifts in the optical line positions with the average strain, involving the a and b parameters only. Moreover, if the strains are determined directly from the x-ray data and the InP values are used for the other material values, there are no free parameters within this model for the samples under study.

The composition dependence of the bulk $Ga_xIn_{1-x}P$ band gap in the low Ga concentration region is defined at low temperatures by[18]

$$E_g(x)=1.423+0.77x+0.648x^2 \text{ (eV)}. \tag{7}$$

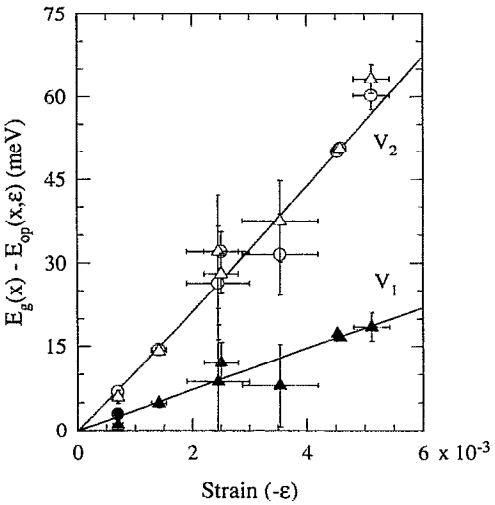

FIG. 6. Strain dependences of the absorption (A_1, open triangles; A_2, full triangles) and PL (P_2, open circles; P_3, full circles) energies [$E_g(x)-E_{op}(x,\epsilon)$, $E_{op}(x,\epsilon)$ corrected for the exciton binding energy]. Solid lines are the calculations of the strain-dependent terms of the heavy-hole (V_1) and light-hole (V_2) band energies from Eqs. (8).

The strain dependence of the heavy- and light-hole band-gap energies at $k=0$ (Ref. 17) can be expressed to second order in ϵ in the following form:

$$E_g(x)-E_g^{\rm hh}(x,\epsilon)=2a\left(\frac{c_{11}-c_{12}}{c_{11}}\right)\epsilon-b\left(\frac{c_{11}+2c_{12}}{c_{11}}\right)\epsilon, \tag{8a}$$

$$E_g(x)-E_g^{\rm lh}(x,\epsilon)=2a\left(\frac{c_{11}-c_{12}}{c_{11}}\right)\epsilon+b\left(\frac{c_{11}+2c_{12}}{c_{11}}\right)\epsilon+\frac{2b^2}{\Delta}\left(\frac{c_{11}+2c_{12}}{c_{11}}\right)^2\epsilon^2. \tag{8b}$$

In applying Eqs. (8), the parameter values (a, b, Δ, and c_{ij}) are chosen to be those for pure InP and are listed in Table II. In our initial analysis we also tried composition-weighted averages of the parameters for InP and GaP but, within the experimental resolution of the data, this choice made no significant difference, due in part to the small values of the Ga concentrations and in part to the similarity of the parameters for the two materials.

In Fig. 6 we demonstrate the excellent agreement between Eqs. (8) and the optical data by plotting the experimental data as $E_g(x)-E_{\rm op}(x)$ versus the average strain ($-\epsilon$). Here $E_g(x)$ is the bulk, relaxed band gap given in Eq. (7) and $E_{\rm op}(x)$ is the measured optical energy corrected for exciton effects by assuming a constant exciton binding energy of 5 meV. For the lower-energy optical absorption transitions in samples CE62*S*, CE63*S*, and CF86*S*, which have the form of an edge absorption rather than an excitonic transition, no binding energy correction has been added. The error bars in the figure are fixed by the uncertainties in calculating the sample composition and strain from the x-ray data. The solid lines represent the right-hand sides of Eqs. (8) for the heavy-hole (V_1) and

light-hole (V_2) bands. Within experimental uncertainty these lines pass through the data points with no adjustable parameters.

Several important deductions can be drawn from the present analysis. No *a priori* assumption has been made about the origin of the various experimental optical transitions. As a result, this analysis clearly identifies the lower-energy peaks in both the optical absorption and PL spectra as transitions between the light-hole and conduction bands; the higher energy peaks arise from transitions between the heavy-hole and conduction bands. This assignment is also in agreement with the relative intensities of the absorption transitions since the corresponding optical transition matrix element for the heavy-hole transition is a factor of 3 greater than that for the light-hole transition. In Fig. 6 the light-hole energy clearly varies about three times more rapidly with strain than the heavy-hole energy. On this basis, nonuniformity of the strain will tend to wash out the light-hole transition more rapidly than the heavy-hole one. Spectra for the most strained samples are consistent with this deduction. Finally, we point out that the low-temperature optical absorption and PL are complementary, providing mutually consistent data for all samples.

V. CONCLUSION

We have reported a detailed investigation of the structural and optoelectronic properties of GaInP epilayers on sulfur-doped InP substrates. These substrates open an optical absorption window through which we have followed the light- and heavy-hole optical absorption in the epilayer in the region above the band gap of undoped InP. Significant variations of the optical absorption and PL transitions from these two bands are observed as a function of the epilayer composition as well as the degree of relaxation of the misfit strain (a maximum shift of more than 60 meV for light holes and 20 meV for heavy holes is observed). Using x-ray measurements to determine the Ga concentration and the strains in each of the samples, the strain-induced shift of both the PL and absorption positions agree remarkably well with the theoretical calculations based on the strain Hamiltonian of Pikus and Bir.[16] This agreement is all the more remarkable since there are no free parameters within the model and serves to identify unambiguously the transitions observed in the optical absorption and PL spectra.

For these thick films both isotropic and anisotropic in-plane strain relaxations are observed. The effect of relaxation is most noticeable on the optical linewidths and intensities where even a very small relaxation results in a significant increase of the linewidth and an even more rapid drop in the transition intensity. It is noted that these characteristics are related to the degree of relaxation and not to the composition nor the lattice mismatch as reported in Ref. 19. Isotropic in-plane relaxation produces a first-order shift of both light- and heavy-hole energies. However, anisotropic relaxation generates a shear strain in the layer plane which contributes only negligibly to the transition energy.

Finally, we point out that such a complete understanding of the optical behavior of relatively thick epitaxial layers, including isotropic and anisotropic strain relaxation, has already proven to be essential for the interpretation of optical spectra from the carriers in confined states in strained-layer superlattices and multiple quantum wells.[20]

ACKNOWLEDGMENTS

This work has been supported by the Natural Sciences and Engineering Research Council of Canada and le Fonds FCAR du Québec. The technical assistance of Laurent Isnard and René Lacoursière has been greatly appreciated. Two of the authors (A. B. and A. C.) would like to acknowledge financial support from the Institute of Physics, University of Oran, Algeria.

[1] A. Bensaada, R. W. Cochrane, R. A. Masut, R. Leonelli, and G. Kajrys, J. Cryst. Growth **130**, 433 (1993); A. Bensaaada, A. Chennouf, R. W. Cochrane, R. Leonelli, P. Cova, and R. A. Masut, J. Appl. Phys. **71**, 1737 (1992).
[2] G. H. Olsen, C. J. Nuese, and R. T. Smith, J. Appl. Phys. **49**, 5523 (1978).
[3] H. Asai and K. Oe, J. Appl. Phys. **54**, 2052 (1983).
[4] C. P. Kuo, S. K. Vong, R. M. Cohen, and G. B. Stringfellow, J. Appl. Phys. **57**, 5428 (1985).
[5] K. Ozasa, M. Yuri, S. Tanaka, and H. Matsunami, J. Appl. Phys. **68**, 107 (1990).
[6] F. Yang, A. Ishida, and H. Fujiyasu, Appl. Phys. Lett. **56**, 2114 (1990).
[7] P. Cova, R. A. Masut, J. F. Currie, A. Bensaada, R. Leonelli, and C. Anh Tran, Can. J. Phys. **69**, 412 (1991).
[8] A. Onton, M. R. Lorentz, and W. Reuter, J. Appl. Phys. **42**, 3420 (1971).
[9] M. Bugajski and W. Lewandowski, J. Appl. Phys. **57**, 521 (1985).
[10] A. Knauer, R. Staske, J. Kraüsslich, and R. Kittner, J. Electron. Mater. **20**, 1095 (1991); J. P. Farges, C. Shiller, and W. J. Bartels, J. Cryst. Growth **83**, 159 (1987).
[11] A. Bensaada, R. W. Cochrane, and R. A. Masut (unpublished).
[12] Chu R. Wie and H. M. Kim, SPIE **877**, 41 (1988).
[13] H. Hasegawa, Phys. Rev. **129**, 1029 (1963); J. C. Hensel and G. Feher, *ibid.* **129**, 1041 (1963).
[14] I. Kudman and R. J. Paff, J. Appl. Phys. **43**, 3760 (1972).
[15] F. H. Pollack, Surf. Sci. **37**, 863 (1973).
[16] G. E. Pikus and G. L. Bir, Sov. Phys. Solid State **1**, 136 (1959); **1**, 1502 (1960).
[17] F. H. Pollak and M. Cardona, Phys. Rev. **172**, 816 (1968).
[18] P. Merle, D. Auvergne, and H. Mathieu, Phys. Rev. B **15**, 2032 (1977).
[19] J. S. Yuan, M. T. Tsai, C. H. Chen, R. M. Cohen, and G. B. Stringfellow, J. Appl. Phys. **60**, 1346 (1986).
[20] A. Bensaada, J. T. Graham, J. L. Brebner, A. Chennouf, R. W. Cochrane, R. Leonelli, and R. A. Masut, Appl. Phys. Lett. **64**, 273 (1994).